Vol 18 No 10, October 2009
1674-1056/2009/18(10)/4443–06

Chinese Physics B

© 2009 Chin. Phys. Soc.
and IOP Publishing Ltd

First-principles calculations for electronic and optical properties of the zinc-blende structured BeS compound under pressure*

Yang Huan(杨 欢)[a)], Chang Jing(常 景)[a)],
Li Zhe(李 哲)[a)], and Chen Xiang-Rong(陈向荣)[a)b)†]

[a)] *Institute of Atomic and Molecular Physics, School of Physical Science and Technology, Sichuan University, Chengdu* 610065, *China*
[b)] *International Centre for Materials Physics, Chinese Academy of Sciences, Shenyang* 110016, *China*

(Received 13 March 2009; revised manuscript received 13 April 2009)

The electronic and the optical properties of the cubic zinc-blende (ZB) BeS under high pressure have been investigated by using *ab initio* plane-wave pseudopotential density functional theory method in the generalised gradient approximation (GGA) for exchange-correlation interaction. The electronic band structure and the pressure dependence of the total and partial densities of state under pressure are successfully described. Our calculations show that the ZB BeS has large and indirect band gaps associated with ($\Gamma \rightarrow X$) transitions in ambient conditions. The results obtained are consistent with the experimental data available and other calculations. The optical properties, including dielectric function, energy-loss function, complex refractive index, reflection and absorption spectra, are investigated and analysed at different external pressures. The results suggest that the optical absorption appears mostly in the ultra-violet region and the curve of refractive index shift toward high energies (blue shift) with pressure increasing.

Keywords: density functional theory, electronic structure, optical properties, high pressure, BeS
PACC: 7115M, 3620K, 4281D, 7470F

1. Introduction

Recently, the wide band-gap II–VI compounds have received considerable attention because of their possible applications in optoelectronic devices.[1−14] Among the II–VI semiconducting AX compounds (A = Be, Mg, Ca, Sr, Ba; X = O, S, Se, Te), the beryllium chalcogenides BeX (X = O, S, Se, Te) have a much high degree of covalent binding, and are characterised by their small ionic radius ratios as compared with other wide-gap II–VI semiconductors. They may be applied to blue–green laser diodes and laser-emitting diodes, and they can be grown on various substrates by molecular beam epitaxy (MBE).[13] It is found that these compounds are partially ionic semiconductors with large and indirect band gaps ($\Gamma \rightarrow X$).

As a semiconductor compound, the zinc-blend (ZB) BeS in an ambient condition has a high value of the bulk modulus, which leads hardness and stability to increase. These interesting properties make them potential materials used in the optoelectronic devices. Recently, several investigations were made on BeS. Kalpana *et al*[11] investigated the structural and electronic properties of BeX (X = O, S, Se, Te) compounds by using the tight-binding linear muffin-tin orbitals method (TB-LMTO). Benosman *et al*,[2] Okoye,[12] El Hadj Hassen and Akbarzedeh[10] reported on the electronic and the optical properties of these compounds. In addition, Rached *et al*[14] obtained the ground state properties and the structural phase transformation of these BeX compounds by using the full-potential linear muffin-tin orbital method (FP-LMTO). More recently, Chang *et al*[3] investigated the elastic and thermodynamic properties of the ZB BeS under high pressures and temperatures.

Presently, many calculations of the band structures have been reported for these compounds in ambient condition, but there are few reports on the band structures of BeX under high pressure. Especially, to our knowledge, there is no study of the effect of pressure on their optical properties. Therefore, the aim

*Project supported by the National Natural Science Foundation of China (Grant No 10776022) and the National Key Laboratory Fund for Shock Wave and Detonation Physics Research of the China Academy of Engineering Physics (Grant No 9140C6711010805).
†Corresponding author. E-mail: x.r.chen@tom.com

of this work is to give a detailed description of the behaviour of electronic and optical properties of the ZB BeS under high pressure. In Section 2, we outline the theoretical framework within which all the calculations have been performed, a detailed description and analysis of our results are displayed in Section 3. Finally, a conclusion of the present study is given in Section 4.

2. Theoretical method

In the electronic structure calculations, the non-local ultrasoft pseudopotentials introduced by Vanderbilt[15] have been employed for all the ion-electron interactions, together with generalised gradient approximation (GGA) for exchange-correlation functional in the scheme of Perdew–Bueke–Ernzerhof (PBE).[16] Pseudo-atom calculations are performed for S $3s^2 3p^4$ and Be $2s^2$. The self-consistent convergence of the total energy is 5.0×10^{-6} eV/atom. To confirm the convergence of our calculations, we carefully investigate the dependences of the total energy on the cutoff energy and the k-point set mesh according to the Monkhorst–Pack grid. Considering the computational cost, a plane-wave basis set with an energy cut-off of 450 eV is applied, and an $8\times8\times8$ k-point Monkhorst–Pack mesh is used for the Brillouin-zone (BZ) k-point sampling. It is found that these parameters are sufficient for leading to well converged total energy.

For the calculation of the optical properties, an appropriate number of k-points in the Brillouin zone (BZ) are required when the optical matrix elements are calculated. Hence, the Brillouin zone integration is performed by using the tetrahedron method with many points more than k-points in the irreducible part of the Brillouin zone without broadening. Thus, to investigate the properties accurately, sufficiently dense k-meshes, which consist of $6\times6\times6$ k-meshes for the ZB BeS, are used. The non-local ultrasoft pseudopotentials introduced by Vanderbilt[15] are adopted all the same. Meanwhile, the number of conduction bands, which determines the energy range covered and the accuracy of the Kramers–Kronig transform, is also an important parameter in the calculation. In the present study, in addition to the occupied bands, 12 empty bands are included, and the electronic structure and optical properties are all studied by using the Cambridge Serial Total Energy Package (CASTEP) code.[17,18]

3. Results and discussion

3.1. Electronic structures of ZB BeS under pressure

BeS is a cubic crystal with space group $F4\text{-}3M$, where Be atom occupies the $4a$ (0, 0, 0) site and S atom occupies the $4c$ (0.25, 0.25, 0.25) site. Firstly, we set a series of different values of lattice constants a to calculate the total energy E and the corresponding primitive cell volume V for the ZB BeS at 0 GPa and 0 K, and then fit the calculated E–V data to the natural strain equation of state (EOS).[19] We obtained the pressure dependence of lattice constants at 0 K. The equilibrium lattice constant a (4.888 Å, 1 Å = 0.1 nm), bulk modulus B_0 (90.04 GPa) and its pressure derivative B_0' (3.7365) are in satisfactory agreement with the experimental data and other theoretical results.[3,8−11,20] On the basis of these results, we further extend our investigation to the electronic band structures and the total density of states (TDOS) along various symmetry lines at 0 GPa and 100 GPa separately. The results obtained are shown in Fig.1, where the top of the valence band is taken as zero energy level. The different symmetry points considered in the BZ are W (from (0.5, 0.25, 0.75) to (0.5, 0.5, 0.5)), Γ (from (0.0, 0.0, 0.0) to (0.5, 0.0, 0.5)), X (from (0.5, 0.0, 0.5) to (0.5, 0.25, 0.75)), K (from (0.5, 0.5, 0.5) to (0.375, 0.375, 0.75)) and L (from (0.5, 0.5, 0.5) to (0.0, 0.0, 0.0)). The overall band profiles are in good agreement with other theoretical results.[1,2,20−23] From Figs.1(a) and 1(b), we can see that the top of valence band (VB) is at Γ-symmetry point and the bottom of conduction band (CB) is at X-symmetry point, which suggests that the ZB BeS has an indirect gap occurring between Γ and X points. Figure 1(a) shows that at 0 GPa, the indirect band gap ($\Gamma_{15V} - X_{1C}$) occurs at 3.23 eV, and the minimum direct gap ($\Gamma_{15V} - \Gamma_{1C}$) occurs at 5.514 eV. The direct and the indirect band gaps together with other theoretical results are present in Table 1. In addition, by comparing the TDOS diagram of Fig.1(a) with that of Fig.1(b), we can find that the TDOS at the edges of the band gap becomes small with pressure increasing, and the valence band of the ZB BeS shifts upwards while the conduction shifts downwards. The peaks descend with the pressure increasing but the bandwidths become broad, which implies that the electrons in those states are active under pressure.

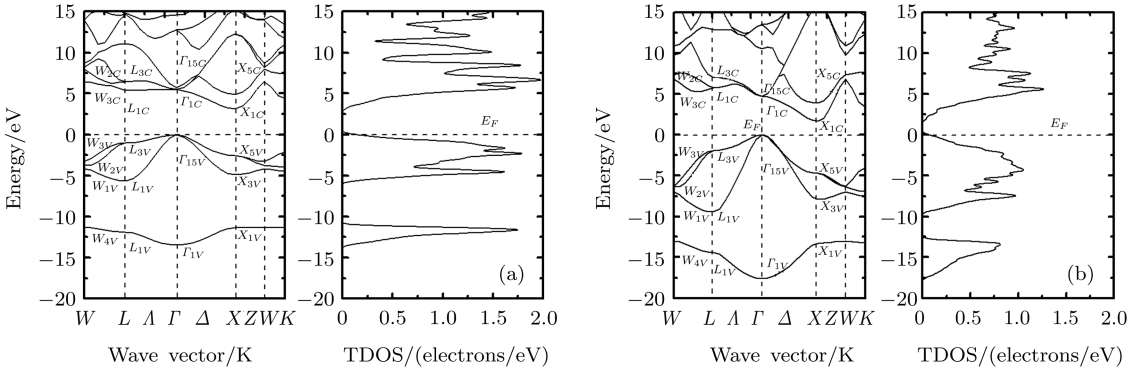


Fig.1. Curves for band structure and total density of states (TDOS) for the ZB BeS at 0 K for (a) 0 GPa and (b) 100 GPa.

Table 1. Important features of band structures for ZB BeS at 0 K and 0 GPa.

	minimum gaps/eV		
	indirect	direct	valence band width/eV
present work	3.23 ($\Gamma_{15V} \to X_{1C}$)	5.514 ($\Gamma_{15V} \to \Gamma_{1C}$)	13.395
GGA[1]	3.11 ($\Gamma_{15V} \to X_{1C}$)	5.51 ($\Gamma_{15V} \to \Gamma_{1C}$)	
FP-LAPW[2]	2.847($\Gamma_{15V} \to X_{1C}$)	5.503 ($\Gamma_{15V} \to \Gamma_{1C}$)	13.80766
LDA[20]	2.75 ($\Gamma_{15V} \to X_{1C}$)	5.51 ($\Gamma_{15V} \to \Gamma_{1C}$)	14.07
LDA[23]	2.816 ($\Gamma_{15V} \to X_{1C}$)	5.397 ($\Gamma_{15V} \to \Gamma_{1C}$)	
OPW[24]	4.17 ($\Gamma_{15V} \to X_{1C}$)		
APW[25]		6.10 (at 0 K)	
expt.[26]		> 5.5	

It is not difficult to find that our results at 0 K and 0 GPa are very close to those obtained by Yim *et al*,[26] Yadav *et al*[1] and Benosman,[2] who performed their calculations by means of the self-consistent full-potential linear-augmented-plane wave method (FP-LAPW) in the local-spin density approximation (LSDA) and a self-consistent manner by using the ABINIT code in the generalized gradient approximation (GGA). The valence bandwidth is equal to 13.395 eV, which is in very good agreement with the value obtained by Yim *et al.*[26] From the TDOS diagram, we can see that the TDOS at the edges of the band gap is small, the minimum density of the states occurs at –11.653 eV, which is similar to those in earlier studies.[1,2] The large peak at 6.716 eV comes primarily from the onset of the second conduction band at the point L.

To investigate the effects of pressure on the electronic structure for the ZB BeS, we also investigate the band structures, the total density of states (TDOS) and the partial densities of states (PDOS) at 0 GPa and 100 GPa, separately. In Table 2, we present the main band gaps and the valence band widths for the ZB BeS at different pressures. It is clear that the indirect gaps ($\Gamma_{15V} - X_{1C}$) and ($L_{3V} - X_{1C}$) and the direct gaps ($\Gamma_{15V} - \Gamma_{1C}$) decrease with pressure increasing from 0 to 100 GPa, while the indirect gap ($\Gamma_{15V} - L_{1C}$) increases with pressure increasing except from 60 GPa to 100 GPa. The direct gap ($L_{3V} - L_{1C}$) increases with the pressure except at 80 GPa, the direct gap ($X_{5V} - X_{1C}$) increases with pressure increasing, but at 60 GPa and 80 GPa the gaps are almost the same. Namely, the prominent direct gaps ($\Gamma_{15V} - \Gamma_{1C}$) and indirect gaps ($\Gamma_{15V} - X_{1C}$) decrease with pressure increasing. Moreover, the valence bandwidth is generally enhanced as pressure increases from 0 to 100 GPa. From the description above, it is found that there is an abnormal phenomenon at about 60 GPa.

The partial density of states (PDOS) of the ZB BeS at 0 GPa and 100 GPa have been plotted in Figs.2(a) and 2(b), respectively, where the Fermi level is set to be 0 point. It is seen that at 0 GPa the peaks of PDOS decrease and extend to flat, which suggests that large hole effective masses and some unusual transport properties may be expected for the

Table 2. Main band gaps (eV), valence band widths (eV) for the ZB BeS at different pressures (GPa).

energy gaps		P					
		0	20	40	60	80	100
direct gaps	$L_{3V}-L_{1C}$	6.40	7.245	7.544	7.656	7.595	7.613
	$\Gamma_{15V}-\Gamma_{1C}$	5.514	5.413	5.207	5.063	4.899	4.671
	$X_{5V}-X_{1C}$	5.864	5.928	6.113	6.267	6.268	6.420
indirect gaps	$\Gamma_{15V}-L_{1C}$	5.381	5.99	6.195	6.02	5.825	5.689
	$\Gamma_{15V}-X_{1C}$	3.230	2.748	2.521	2.233	1.884	1.636
	$L_{3V}-X_{1C}$	4.249	4.003	3.87	3.869	3.654	3.560
valence band widths		13.395	14.654	15.478	16.414	16.918	17.654

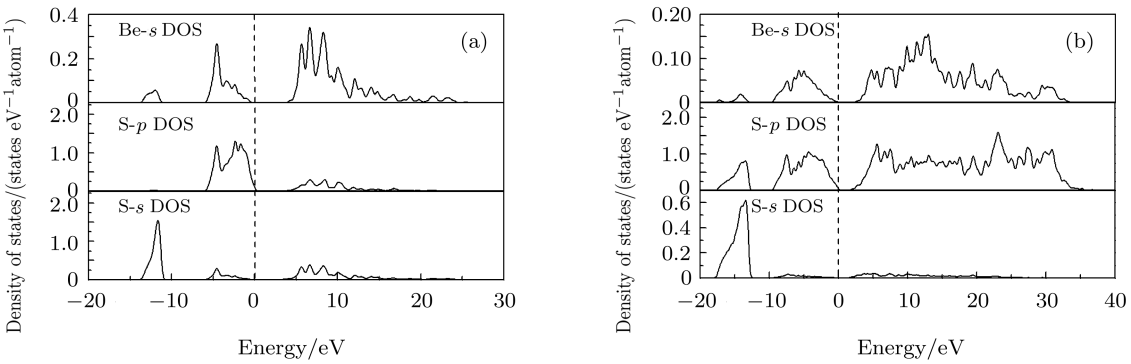


Fig.2. Curves for partial density of states (PDOS) of ZB BeS for Be-2s, S-3p, and S-3s at 0 K for (a) 0 GPa and (b) 100 GPa.

p-type semiconductor. For the PDOS at 100 GPa, it is found that the peaks of Be 2s and S 3p increase and extend to high energies, but the S 3s decreases. This can be understood as that the S 3p and the Be 2s electrons in those states are active under pressure because of the increasing of overlap between the bonds and the changed hybridization. In addition, the valence band is mainly composed of p electron while the conduction band is composed of the hybrid s and p electrons.

3.2. Optical properties of ZB BeS under pressure

To further understand the ZB BeS under pressure, we also investigate the optical properties, which include many physical parameters, such as the frequency-dependent complex dielectric constant $\varepsilon(\omega)$, the electron energy loss function $L(\omega)$, the refractive index $n(\omega)$, the absorption coefficient $I(\omega)$, the reflectivity coefficient R, the extinction coefficient $k(\omega)$, the optical conductivity σ, and so on. All of these parameters are connected with each other and can be derived from the real part $\varepsilon_1(\omega)$ and the imaginary part $\varepsilon_2(\omega)$ of the dielectric function, which is known to describe the optical response of the medium at all photon energies $E = h\omega$, by using the formalism of Ehrenreich and Cohen.[27] All the optical constants obtained are shown in Fig.3. Furthermore, the imaginary part $\varepsilon_2(\omega)$ in the long wavelength limit has been obtained directly from the electronic structure calculation, also it can be obtained from the momentum matrix elements between the occupied and the unoccupied wave functions within the selection rules, together with the Kramer–Kronig relationship.

In Fig.3(a), we display the dielectric function curves for the photon energy ranging from 0 eV to 30 eV at 0 GPa and 100 GPa separately. It can be seen that in a high-energy area (frequency larger than 20 eV), the values of the imaginary part are very small, while the real part changes very little for the ZB BeS. In real part curve at 0 GPa, there is an obvious peak at 5.808 eV, it is due to the direct interband transitions

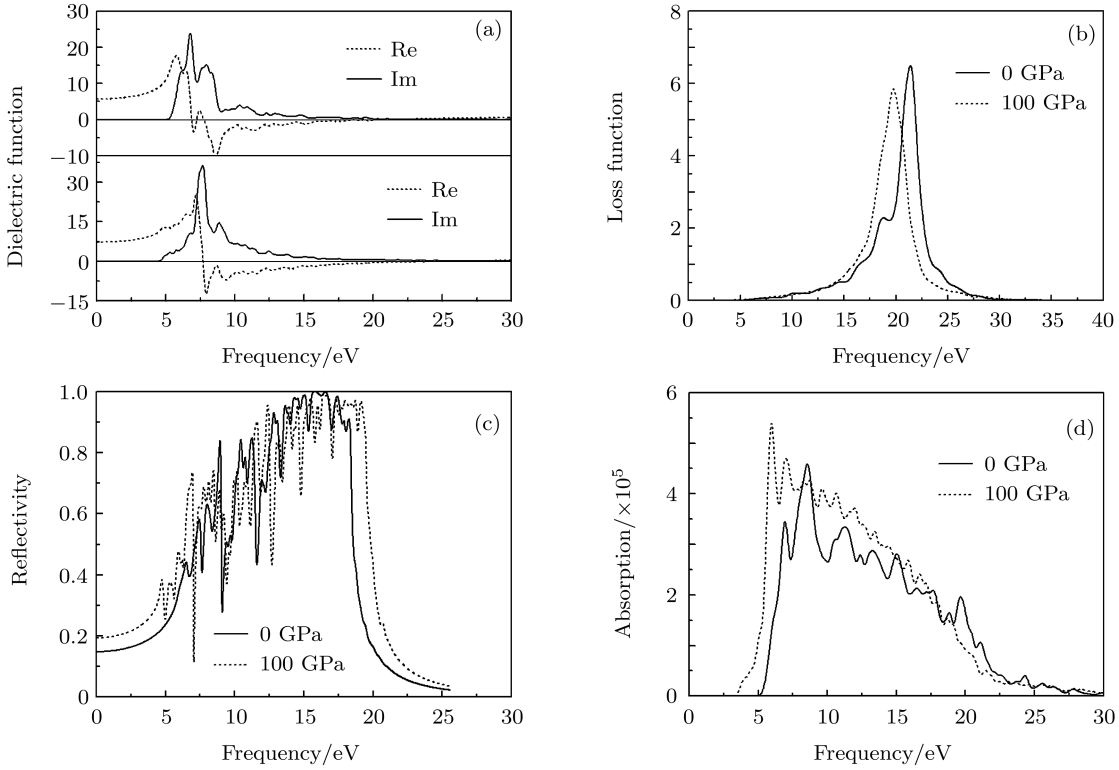


Fig.3. Optical properties of the ZB BeS. The instrumental smearing for Gaussian broadening is specified by an identical value 0.5. Panel (a) is for dielectric function, panel (b) for loss function, panel (c) for reflectivity, and panel (d) for absorption spectra.

which originate from the top of the valence band at the L-point to the lowest conduction band. Subsequently, a sharp reduction comes. However, the highest peak in real part curve decreases with pressure increasing. For the imaginary part of the dielectric function, there also exists such a similar descent, that is, the highest peak in imaginary part curve also decreases with pressure increasing. Many direct or indirect transitions may be found in the band structure with an energy corresponding to the same peak. Thus, the peak in imaginary part $\varepsilon_2(\omega)$ does not correspond to a single interband transition. The electron energy-loss function $L(\omega)$, which is an important factor describing the energy loss of a fast electron traversing in the material, is displayed in Fig.3(b) for the ZB BeS at 0 GPa and 100 GPa. It can be seen that the prominent peak of $L(\omega)$ decreases and shifts towards the high energies with pressure increasing, and it corresponds to the trailing edges of the reflection spectra shown in Fig.3(c) when the reflectivity reduces sharply. A comparison between Fig.3(c) and Fig.3(d) indicates that the relationships corresponding to reflection and absorption spectra are similar to each other. That means if a kind of material can absorb light in some range strongly, it can also effectively reflect the light in the same range. The absorption spectrum has an absorption band in a low energy range, and the strong optical absorption appears mostly in the ultra-violet region which corresponds to the interband transitions. However, the absorption decreases with the photon energy in a high energy range, where the electron is hard to respond.

Finally, we study the influence of pressure on the complex refractive index among optical properties for the ZB BeS. In Fig.4, both the real and the imaginary parts of complex refractive index at different pressures are illustrated. It is clearly seen that in a high-energy area, where the frequency of photons is corresponding to the energy larger than 20 eV, the values of the imaginary part are very small, while the values of the real part change very little for the ZB BeS. This means that the absorption of the high frequency electromagnetic wave is very weak and the refractive index is almost constant in the high frequency area. In a low energy area, where the photon energy is less than 5 eV, the imaginary part is almost zero and the real part is almost constant, which suggests that the optical absorption appears mostly in the ultra-violet region, and

there are sharp peaks in the low energy area at about 6.948 eV and 8.6 eV, separately. By comparison, it can be seen that the pressure has little effect on the shape of the refractive index curve, but the positions of the peaks shift toward higher energies as shown by the arrows in Fig.4.

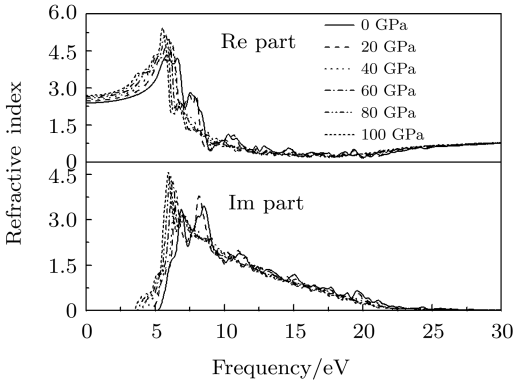


Fig.4. Curves for refractive index of ZB BeS at different external pressures.

4. Conclusions

We use the *ab initio* plane-wave pseudopotential density functional theory method in the generalized gradient approximation (GGA) for exchange-correlation interaction to study the structure, the electronic and the optical properties of ZB BeS. Our results are in good agreement with the available experimental data and other theoretical results. An indirect band gap induced by the $(\Gamma \rightarrow X)$ transition is presented, with its value being 3.230 eV. The band calculations are comparable to available measurements very well. In addition, we reveal different behaviours of TDOS and PDOS of the ZB BeS under high pressure. The obtained optical parameters, including the dielectric constant, the electron energy loss function, the refractive and the absorption indexes, suggest that the strong absorption spectrum appears mostly in the ultra-violet region, and the optical absorption decreases with photon energy in the high energy range.

References

[1] Yadav P S, Yadav R K, Agrawal S and Agrawal B K 2007 *Physica* E **36** 79

[2] Benosman N, Amrane N, Mecabih S and Aourag H 2001 *Physica* B **304** 214

[3] Chang J, Chen X R, Zhang W and Zhu J 2008 *Chin. Phys.* B **17** 1377

[4] Chen X R, Li X F, Cai L C and Zhu J 2006 *Solid State Commun.* **139** 246

[5] Zhao J Z, Lu L Y, Chen X R and Bai Y L 2007 *Physica* B **387** 245

[6] Cheng Y, Lu L Y, Jia O H and Chen X R 2008 *Chin. Phys.* B **17** 1355

[7] Heciri D, Beldi L, Drablia S, Meradji H, Derradji N E, Belkhir H and Bouhafs B 2007 *Comput. Mater. Sci.* **38** 609

[8] Khenata R, Bouhemadou A, Hichour M, Baltache H, Rached D and Rerat M 2006 *Solid State Electronics* **50** 1382

[9] Rached D, Rabah M, Benkhettou N, Khenata R, Soudini B, Al-Douri Y and Baltache H 2006 *Comput. Mater. Sci.* **37** 292

[10] El Haj Hassan F and Akbarzadeh H 2006 *Comput. Mater. Sci.* **35** 423

[11] Kalpana G, Pari G, Mookerjee A and Bhattacharyya A K 1998 *Int. J. Mod. Phys.* B **12** 1975

[12] Okoye C M I 2003 *Eur. Phys. J.* B **39** 5

[13] Waag A, Fischer F, Lugauer H J, Litz Th, Laubender J, Lunz U, Zehnder U, Ossau W, Gerhardt T, Moller M and Landwehr G 1996 *J. Appl. Phys.* **80** 792

[14] Rached D, Rabah M, Benkhettou N, Khenata R, Soudini B, Al-Douri Y and Baltache H 2006 *Comput. Mater. Sci.* **37** 292

[15] Vanderbilt D 1990 *Phys. Rev.* B **41** 7892

[16] Perdew J P, Burke K and Ernzerhof M 1996 *Phys. Rev. Lett.* **77** 3865

[17] Payne M C, Teter M P, Allen D C, Arias T A and Joannopoulos J D 1992 *Rev. Mod. Phys.* **64** 1045

[18] Milan V, Winker B, White J A , Packard C J, Payne M C, Akhmatskaya E V and Nobes R H 2002 *Int. J. Quantum Chem.* **77** 85

[19] Poirier J P and Tarantola A 1998 *Phys. Earth Planet Int.* **109** 1

[20] Gonzalez-Diaz M, Rodriguez-Hernandez P and Munoz A 1997 *Phys. Rev.* B **55** 14043

[21] Fleszar A and Hanke W 2000 *Phys. Rev.* B **62** 2466

[22] Nagelstrasser M, Droge H, Steinruck H P, Fischer F, Litz T, Waag A, Landwehr G, Fleszar A and Hanke W 1998 *Phys. Rev.* B **58** 10394

[23] Van Camp P E and Van Doren V E 1996 *Solid State Commun.* **98** 741

[24] Stukel D J 1970 *Phys. Rev.* B **2** 1852

[25] Sarkar R L and Chettarjee S 1977 *J. Phys.* C **10** 57

[26] Yim W M, Dismukes J P, Stofko E J and Poff R J 1972 *J. Phys. Chem. Solids* **33** 501

[27] Ehrenreich H and Cohen M L 1959 *Phys. Rev.* **115** 786